The Thirty-Second AAAI Conference
on Artificial Intelligence (AAAI-18)

Training L_1-Regularized Models with Orthant-Wise Passive Descent Algorithms

Jianqiao Wangni
Tencent AI Lab
Shenzhen, China
zjnqha@gmail.com

Abstract

The L_1-regularized models are widely used for sparse regression or classification tasks. In this paper, we propose the orthant-wise passive descent algorithm (OPDA) for optimizing L_1-regularized models, as an improved substitute of proximal algorithms, which are the standard tools for optimizing the models nowadays. OPDA uses a stochastic variance-reduced gradient (SVRG) to initialize the descent direction, then apply a novel alignment operator to encourage each element keeping the same sign after one iteration of update, so the parameter remains in the same orthant as before. It also explicitly suppresses the magnitude of each element to impose sparsity. The quasi-Newton update can be utilized to incorporate curvature information and accelerate the speed. We prove a linear convergence rate for OPDA on general smooth and strongly-convex loss functions. By conducting experiments on L_1-regularized logistic regression and convolutional neural networks, we show that OPDA outperforms state-of-the-art stochastic proximal algorithms, implying a wide range of applications in training sparse models.

Introduction

The machine learning community has been favouring L_1-regularized models like logistic regression and linear regression to build robust applications with high dimensional data (Friedman, Hastie, and Tibshirani 2001)(Candes and Tao 2007)(Bach et al. 2012)(Bühlmann and Van De Geer 2011). To process the rapidly increasing scale of internet data, many algorithms were proposed to speed up the training process (Efron et al. 2004)(Zhang 2011)(Nesterov 2013). One of most representative optimization method is the proximal algorithm (Parikh, Boyd, and others 2014), which sequentially takes a gradient descent step and then solves a proximal problem on the current parameter.

When the data number is very large, the stochastic gradient descent algorithm (SGD) (Zhang 2004)(Bottou 2010)(Shamir and Zhang 2013), as opposed to batch algorithms, updates parameters by processing data mini-batches with a higher frequency and minimizes the loss function in expectation, being especially suitable for problems with large condition numbers. However, SGD generally needs a decreasing stepsize to reduce the variance of gradients, and only yields a sublinear convergence rate. Recently, some variance-reduced stochastic algorithms, such as SVRG (Johnson and Zhang 2013) and SAGA (Defazio, Bach, and Lacoste-Julien 2014), can converge without decreasing stepsizes and achieve linear convergence rates on smooth and strongly-convex problems; they can converge at similar rates on L_1-regularized problems if combined with proximal algorithms (Shalev-Shwartz and Zhang 2014)(Xiao and Zhang 2014)(Reddi et al. 2016).

Another promising line of research is about the (quasi) Newton algorithm, which has been popular for decades. It captures more curvature information than first-order algorithms do. It is theoretically guaranteed and practically proved to converge faster, especially when the data dimension is relatively low (Nocedal and Wright 1999). L-BFGS (Liu and Nocedal 1989) circumvents the inversion of Hessian matrices by matrix-vector multiplications, consuming less memory, fitting well with high dimensional data.

Due to the non-differentiability, the L_1-regularized sparse models can not directly benefit from the fast convergence of quasi-Newton algorithms. A representative adaptation of L-BFGS for the problem is the orthant-wise limited memory quasi-Newton method (OWL-QN)(Andrew and Gao 2007). OWL-QN fits this problem uniquely by generalizing L-BFGS and adopting three gradient alignment steps, which make the parameters remain in the same orthant after updates, and defeated other major algorithms on solving L_1-regularized logistic regression, in comparisons conducted by (Yu et al. 2010). Later improved OWL-QN algorithms (Gong and Ye 2015a)(Gong and Ye 2015b) take a hybrid approach of OWL-QN updates and proximal gradient descent steps, proving a theoretical convergence for a family of non-convex models with nonconvex regularizations.

The success of SGD has led to some progresses toward stochastic quasi-Newton algorithms (SQN) that employ subsampled gradients as initializations (Schraudolph et al. 2007). The regularized SQN (Mokhtari and Ribeiro 2014) further added an identity matrix to the inverse Hessian matrix to guarantee the positive-definiteness. (Moritz, Nishihara, and Jordan 2016) proposed a linear convergent SQN with SVRG initializing descent directions.

Inspired by the aforementioned research, in this paper, we proposed an efficient but simple algorithm for L_1-regularized problems. We propose a generalization of the

alignment operator from OWL-QN, and use SVRG for initializing the descent direction. We also present multiple strategies for calculating the quasi-Newton direction. The algorithm is evaluated on both convex and nonconvex problems, and the experiments demonstrate a significant improvement upon the proximal algorithms.

Preliminaries

We study the regularized function $P(x)$ on $x \in \mathbb{R}^D$ as

$$P(x) = F(x) + R(x), \tag{1}$$

where F is the average of N loss functions, each of which depends on a data sample, and R is the L_1 regularization,

$$F(x) = \frac{1}{N}\sum_{i=n}^{N} f_n(x), \quad R(x) = \lambda||x||_1. \tag{2}$$

Assumption 1. Each loss function $f_n : \mathbb{R}^D \to \mathbb{R}$ is twice differentiable, μ-strongly-convex, and has L-Lipschitz continuous gradient (L-smoothness), such that

$$\mu I_D \preceq \nabla^2 f_n(x) \preceq L I_D, \quad \forall 1 \le n \le N \tag{3}$$

where $||\cdot||$ is Euclidean norm, $0 < \mu \le L$ and $I_D \in \mathbb{R}^{D\times D}$ is an identity matrix. Their finite average $F(x)$ also satisfies the smoothness and the strong convexity.

Definition 2. A proximal gradient algorithm for the problem in Eq.(1) sequentially finds a minimum on a quadratic expansion at $x_{k-1} \in \mathbb{R}^D$ in the k-th step,

$$x_k = \underset{x\in\mathbb{R}^D}{\operatorname{argmin}} \nabla F(x_{k-1})^\top x + \frac{1}{2\eta}||x - x_{k-1}||^2 + R(x), \tag{4}$$

where η is the stepsize. This step can be written as

$$x_k = \mathit{prox}_{\eta R}(x_{k-1} - \eta\nabla F(x_{k-1})), \tag{5}$$

by a proximal operator

$$\mathit{prox}_{\eta R}(y) = \underset{x\in\mathbb{R}^D}{\operatorname{argmin}} \frac{1}{2}||x - y||^2 + \eta R(x). \tag{6}$$

For L_1 regularization $R(x) = \lambda||x||_1$, there is

$$\mathit{prox}_{\eta R}(x) = \operatorname{sign}(x) \odot \max(|x| - \eta\lambda, 0), \tag{7}$$

where $\odot$ is the element-wise product.

Orthant-Wise Quasi Newton Method (OWL-QN). The algorithm (Andrew and Gao 2007) restricts the updated parameter to be within certain orthants to keep differentiability of the L_1-regularized problem. We denote the sign function $\sigma()$ as follows: $\sigma(x_i) = 1$, if $x_i > 0$; $\sigma(x_i) = -1$ if $x_i < 0$ and $\sigma(x_i) = 0$ for otherwise. The alignment operator $\pi : \mathbb{R}^D \to \mathbb{R}^D$ is defined by per element as

$$\pi_i(x; y) = \begin{cases} x_i, & \mathit{if} \quad \sigma(x_i) = \sigma(y_i), \\ 0, & \mathit{otherwise}, \end{cases} \tag{8}$$

where $y \in \mathbb{R}^D$ provides a reference orthant and y_i is the i-th element of y. The alignment operator enforces two elements to have the same sign, so the two vectors are in the same orthant. For notation simplicity, we define an element-wise operator $\psi : \mathbb{R}^D \to \mathbb{R}^D$ as

$$\psi_i(v; x; \lambda) = \begin{cases} v_i + \lambda, & \mathit{if} \quad x_i > 0 \\ v_i - \lambda, & \mathit{if} \quad x_i < 0 \\ v_i + \lambda, & \mathit{if} \quad x_i = 0, v_i + \lambda < 0 \\ v_i - \lambda, & \mathit{if} \quad x_i = 0, v_i - \lambda > 0 \\ 0, & \mathit{otherwise}. \end{cases} \tag{9}$$

OWL-QN aligns the pseudo-gradient $\diamondsuit F(x)$ based on the current gradient $\nabla F(x)$ and the parameter x,

$$\diamondsuit F(x) = \psi(\nabla F(x); x; \lambda). \tag{10}$$

Then, by minimizing an approximated quadratic expansion at point x_{k-1} of Eq.(1), OWL-QN finds a direction d_k as

$$\begin{aligned} d_k &= -\underset{d\in\mathbb{R}^D}{\operatorname{argmin}} F(x_{k-1}) + \diamondsuit F(x_{k-1})^\top d + d^\top B_k d/2 \\ &= H_k \diamondsuit F(x_{k-1}), \end{aligned}$$

where B_k is an approximated Hessian matrix at $x = x_{k-1}$ and $H_k = B_k^{-1}$. OWL-QN applies H_k to obtain a quasi-Newton direction d_k, then takes the second alignment to obtain a direction p_k which is orthant-wise equal to $\diamondsuit F(x)$,

$$p_k = \pi(d_k; \diamondsuit F(x^k)). \tag{11}$$

After this step, OWL-QN makes the third alignment, which explicitly restricts the updated parameter $x_{k-1} - \alpha_k p_k$ to be in the same orthant with x_{k-1}, as

$$x_k = \pi(x_{k-1} - \alpha_k p_k; x_{k-1}), \tag{12}$$

where the optimal stepsize α_k is obtained by line-searching.

The Proposed Algorithm

Although being practically efficient, the aforementioned OWL-QN can certainly be further modified for possible improvement, for examples, by eliminating the line-search procedure, or using subsampled gradients instead of accurate but costly full gradients. Another promising research that attracts us is the stochastic variance-reduced gradient algorithm (SVRG)(Johnson and Zhang 2013), which adds a full gradient on a reference point to the subsampled gradient, and balances the gradient expection by substracting a subsampled reference gradient evaluated on the same subset. It converges well with a constant stepsize, and achieves a linear convergent rate for strongly-convex case. Inspired by SVRG and OWL-QN, we develop an improved algorithm that specializes in optimizing L_1-regularized problems. It combines the variance reduction technique of SVRG with the alignment operator of OWL-QN, but with a relative passive orthant-wise restriction on the parameter. We refer to it as the orthant-wise passive descent algorithm (OPDA).

Definition 3. A subsampled loss function f_k in the k-th step is evaluated on a subset S_k, that

$$f_k(x) = \frac{1}{|S_k|}\sum_{n\in S_k} f_n(x), \quad \text{where} \quad S_k \subset \{1, ..., N\}. \tag{13}$$

The stochastic variance-reduced gradient (SVRG) v_k is as

$$v_k = \nabla f_k(x_{k-1}) - \nabla f_k(\tilde{x}) + \nabla F(\tilde{x}), \tag{14}$$

where $\tilde{x} = x_{k'}$ is a reference point obtained in a previous iteration $k'(k' < k)$, where the full gradient $\nabla F(\tilde{x})$ is calculated.

A combination of OWL-QN and SVRG seems simple, this, however, raises many non-trivial difficulties for us to address. The alignment operation sabotages the convergence property, being the main reason for OWL-QN not easy to prove within a decade.

Remark 1. For a modified OWL-QN that uses $d_k = H_k v_k$ as the descent direction, where v_k is a stochastic gradient, we define the actual descent direction in the k-th step as q_k, then

$$\begin{aligned} &\mathbb{E}[P(x_k)] = \mathbb{E}[P(x_{k-1} - \eta q_k)] \qquad (15) \\ \leq\ & F(x_{k-1}) - \eta \nabla F(x_{k-1})^\top q_k + \tfrac{\eta^2}{2}\mathbb{E}[||q_k||^2] + R(x_k). \end{aligned}$$

The key to establish an optimizer that converges fast both in theory and application is to make q_k as an unbiased estimate of $\partial P(x_{k-1})$, and to control the second-order moment $\mathbb{E}[||q_k||^2]$. OWL-QN suggests that

$$\begin{aligned} p_k &= \pi(H_k(v_k + \partial R(x_{k-1})), v_k + \partial R(x_{k-1})), \\ q_k &= (x_{k-1} - \pi(x_{k-1} - \eta p_k, x_{k-1}))/\eta. \end{aligned}$$

As the algorithm approaches a stationary point, v_k approaches the true gradient, as $v_k \to \nabla F(x_{k-1})$, supposing that $0 < \gamma, \gamma I_D \preceq H_k$ is positive-definite, and denoting $\bar{v}_k = \partial P(x_{k-1})$, then the key proposition of OWL-QN (Andrew and Gao 2007)

$$\bar{v}_k^\top q_k \geq \bar{v}_k^\top p_k \geq \bar{v}_k^\top H_k \bar{v}_k \geq \gamma ||\bar{v}_k||^2, \tag{16}$$

which is important for bounding the second term in Eq.(15), does not hold for the case.

The reasons for such a difficulty were originally discussed in (Gong and Ye 2015b), and their solution was to add proximal gradient descent steps to ensure the convergence. The analysis encourages us to modify the gradient alignment operation to ensure a straightforward convergence. To develop our algorithm, we propose the following propositions to define the aligned gradients, descent directions and orthant-wise updates, which are useful to describe OPDA.

Proposition 4. OPDA uses SVRG v_k from Eq.(14) as the initializing descent direction, and uses the following pseudo-gradient to provide a reference orthant for v_k,

$$\diamondsuit f_k(x_{k-1}) = \psi(\nabla f_k(x_{k-1}), x_{k-1}, \lambda), \tag{17}$$

where λ is the regularization parameter in Eq.(1).

Remark 2. Although a more straightforward choice is to set $v_k = \diamondsuit f_k(x_{k-1})$, but this will introduce a non-decreasing variance and compromise the convergence rate.

Next, we take the second alignment step, using the pseudo-gradient $\diamondsuit f_k(x_{k-1})$ as a reference point. This introduces a much smaller bias to v_k, since the two vectors are random with respect to each other.

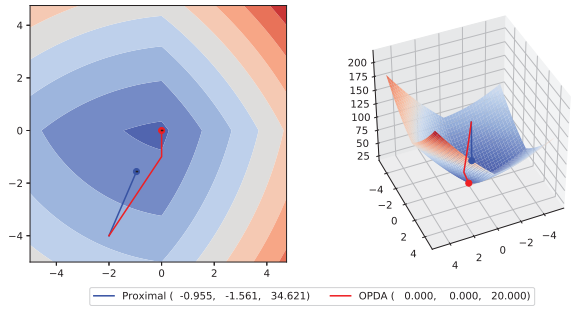

Figure 1: $P(x) = (x_1 + 4)^2 + (x_1 + 2)^2 + 10||x||_1$.

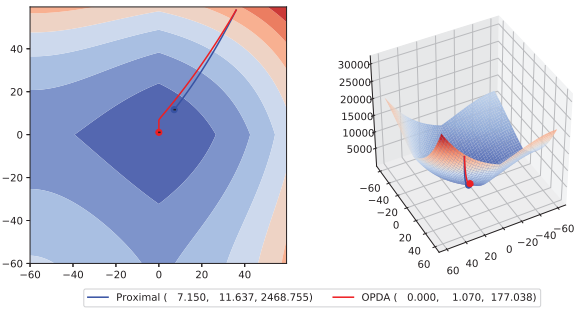

Figure 2: OPDA-FM and a proximal algorithm optimize $P(x) = (x_1 + 4)^2 + (x_1 + 2)^2 + 0.1x_1x_2 + 0.02x_1^3 + 0.02(x_2 + 12)^3 + 100||x||_1$. (Two algorithms have the same stepsize and maximum iteration)

Proposition 5. The descent direction p_k is defined as

$$p_k = \pi(H_k v_k, \diamondsuit f_k(x_{k-1})), \tag{18}$$

where H_k can be obtained from quasi-Newton methods or simply setting to be an identity matrix (first-order).

The aforementioned calculation does not explicitly involve the partial derivative of $R(x)$, except for the alignment reference, since we are avoiding additional variances. To make the solution path to be sparse, we introduce a novel alignment operator to encourage zero elements.

Proposition 6. The orthant-wise alignment operator ϕ is defined as

$$\phi_i(x; y; \varrho) = \begin{cases} 0, & \text{if} \quad \sigma(x_i)\sigma(y_i) = -1 \quad \text{or} \quad |x_i| < \varrho \\ x_i - \varrho\, \text{sign}(x_i), & \text{otherwise}. \end{cases}$$

Remark 3. It is a generalization of $\pi(\cdot)$ operator with a flexible parameter ϱ. it reduces the absolute values of large elements and forces small elements to be zero.

Proposition 7. OPDA updates the parameter and aligns it, based on the aligned direction p_k scaled with a stepsize η,

$$\begin{aligned} x_k &= \phi(x_{k-1} - \eta p_k; x_{k-1}; \eta\lambda), \\ q_k &= (x_{k-1} - x_k)/\eta. \end{aligned}$$

Remark 4. Different from OWL-QN, OPDA allows the update of any element of x_{k-1} from zero to any orthant validated. Each element $p_i, i \in [D]$ of the descent direction p, is

forced to zero if and only if $\sigma(p_i)\sigma(v_i) = -1$. OPDA drives the parameter passively across one orthant to another.

In conclusion, OPDA sequentially calculates the gradient v, the reference orthant $\sigma(\diamondsuit f(x))$, the direction p and the actual update q, as the propositions above. We describe the whole framework in Algorithm 1. Throughout the following paper, we refer to OPDA that $d_k = v_k$ as OPDA-FM (the first-order method), refer to the one that $d_k = H_k v_k$ as OPDA-QN (quasi-Newton). To visualize a comparison, we plot the optimization trajectories of OPDA against a proximal algorithm on a synthetic function in Figures 1&2.

Algorithm 1 Orthant-Wise Passive Descent Algorithms

Input $x_0 \in \mathbb{R}^D$, stepsize $\eta > 0$, and reference points update frequency m.
Initialize $k = 0$, $H_0 = I$, $t = 0$.
repeat
  Compute a full gradient $\nabla F(\tilde{x}_t)$ on the reference point.
  repeat
    Sample a random mini-batch $\mathcal{S}_k \subset \{1, \cdots, N\}$.
    Align the gradient $\diamondsuit f_k(x_{k-1})$ as Eq.(17).
    Compute the subsampled gradient v_k as Eq.(14).
    Choice 1 (OPDA-QN): Compute the direction $d_k = H_k v_k$ via Algorithm 2 or via L-BFGS as Eq.(21).
    Choice 2 (OPDA-FM): Set the direction $d_k = -v_k$.
    Align the direction $p_k = \pi(d_k; \diamondsuit f_k(x))$.
    Align the update $x_k = \phi(x_{k-1} - \eta p_k; x_{k-1}; \eta\lambda)$. Set $k = k + 1$.
  until $k\%m == 0$
  Choice 1: Set $\tilde{x}_{t+1} = \frac{1}{m}\sum_{j=k-m}^{k} x_j$
  Choice 2: Set $\tilde{x}_{t+1} = x_j$, where j is selected uniformly at random from $[m] = \{k - m, k - m + 1, \cdots k\}$.
  Update Hessian matrix H_k as Eq (21), and set $t = t+1$.
until Reaching maximum outer iterations $t = T$, or converging.

Quasi-Newton Updates

For calculating the direction $d = Hv$, we can adopt the method of L-BFGS, where the inverse Hessian approximation H_k is constructed from the curvature pairs (s_j, y_j),

$$s_j = x_j - x_{j-1}, \quad y_j = \nabla F(x_j) - \nabla F(x_{j-1}) \tag{19}$$

for $j \leq k$. Denoting $\rho_j = 1/s_j^\top y_j$, initializing

$$H_k^{k-M} = (s_r^\top y_r / ||y_r||^2) I_D, \tag{20}$$

then OWL-QN recursively computes

$$H_k^j = (I - \rho_j s_j y_j^\top)^\top H_k^{j-1}(I - \rho_j s_j y_j^\top) + \rho_j s_j s_j^\top \tag{21}$$

for $k - M + 1 \leq j \leq k$, and assigns $H_k \leftarrow H_k^k$ as L-BFGS does. We can also incorporate a block BFGS method (Gower, Goldfarb, and Richtárik 2016) to accelerate calculating the direction Hv. This method is derived from L-BFGS, and it solves a linear system which is based on H_{k-1} to obtain H_k,

$$H_k = \underset{H \in \mathbb{R}^{D\times D}}{\operatorname{argmin}} ||(H - H_{k-1})\nabla^2 f_k(x_{k-1})||_F^2, \tag{22}$$

$$s.t. \quad H\nabla^2 f_k(x_{k-1})\Xi_k = \Xi_k; H = H^\top, \tag{23}$$

where $||\cdot||_F$ is the Frobenius norm. The matrix Ξ_k hereby introduces randomness into the algorithm, acting as a sketching function. The system has a closed form solution as

$$\Delta_k = (\Xi_k^\top Y_k)^{-1}, \qquad Y_k = \nabla^2 f_k(x_{k-1})\Xi_k,$$
$$H_k = \Xi_k \Delta_k \Xi_k^\top + (I - \Xi_k \Delta_k Y_k^\top) H_{k-1} (I - Y_k \Delta_k \Xi_k).$$

There are several kinds of random sketching strategies (Gower, Goldfarb, and Richtárik 2016), as follows: a) Ξ_k is an identity matrix; b) each element of Ξ_k is i.i.d sampled from a Gaussian distribution; c) stacks previous unaligned direction vectors as $\Xi_k = [d_{k+1-M}^\top, \cdots, d_k^\top]$.

We describe the matrix-vector multiplication for block BFGS in Algorithm 2. The update frequency of the reference point is indicated by m, which also indicates the times of evaluating subsampled gradients with the same full gradient $\nabla F(\tilde{x})$. The inverse Hessian H_k is updated by every M iterations, and uses M saved (s_j, y_j) curvature pairs (L-BFGS) (Byrd et al. 2016) or (Ξ_j, Y_j, Δ_j) curvature triples (BL-BFGS)(Gower, Goldfarb, and Richtárik 2016). Algorithm 2 consumes $M(4D+2r)r$ arithmetic operations in total. Its cost is approximately $\mathcal{O}(D^{3/2})$ following the setting of (Gower, Goldfarb, and Richtárik 2016) that $r \leq \sqrt{D}$. The calculation of $\Xi_k^\top Y_k$ and the Cholesky factorization results in additional $\mathcal{O}(r^2 D)$ plus $\mathcal{O}(r^3)$ operations. The gradient alignment only consumes $\mathcal{O}(D)$ operations, which are negligible compared to the major costs.

Algorithm 2 Block L-BFGS update

Input $v_k \in \mathbb{R}^D$, $\Xi_j, Y_j \in \mathbb{R}^{D\times r}$ and $\Delta_j \in \mathbb{R}^{r\times r}$ from Algorithm 1, for $j \in \{k + 1 - M, \cdots, k\}$.
Sample a matrix $\Xi_k \in \mathbb{R}^{D\times r}$ that $rank(\Xi_k) = r$.
Compute $Y_k = \nabla^2 f(x_k)\Xi_k$ and $\Xi_k^\top Y_k$.
Compute $\Delta_k = (D_k^\top Y_k)^{-1}$ by Cholesky factorization.
Initialize $v' = v_k$, $j = k$,
Repeat $\alpha_j = \Delta_j \Xi_j^\top v'$, $v' = v' - Y_j v'$, $j = j - 1$, until $j = k - M + 1$.
Repeat $\beta_j = \Delta_j Y_j^\top v'$, $v' = v' + \Xi_j(\alpha_j - \beta_j)$, $j = j + 1$, until $j = k$.
Output: $v' = H_k v_k$.

Convergence Analysis

The difficulty of proving the convergence of an stochastic orthant-wise algorithm mainly rises from the two points: a), (for OPDA-QN) controlling the variance of the descent direction based on an inaccurate gradient. b) dealing with inconsistant orthant-wise constraints from alignment operators. The former issue is shared by all previous stochastic quasi-Newton (SQN) methods (Byrd et al. 2016)(Moritz, Nishihara, and Jordan 2016)(Gower, Goldfarb, and Richtárik 2016)(Luo et al. 2016)(Wang et al. 2017), even with smooth functions. Until now, the variance of the SQN descent direction can only be loosely bounded, therefore they there is no better convergence rate the best first-order methods. Although this drawback is critical, it is not in the scope of this paper. In this section, we follow analyses from (Xiao and Zhang 2014) (Reddi et al. 2016). First,

we define the suboptimality function Q as

$$Q(x) = P(x) - P(x_\star), \quad \text{where} \quad x_\star = \arg\min_x P(x).$$

Then we introduce several lemmas before proceeding to the main theorems.

Lemma 8. For OPDA with Assumption 1 holding, then

$$\mathbb{E}[||\nabla f_k(x) - \nabla f_k(x_\star)||^2] \leq 2LQ(x), \tag{24}$$

Lemma 9. For OPDA with Assumption 1 holding, we set v_k as Eq.(14), then

$$\mathbb{E}[||v_k - \nabla F(x_{k-1})||^2] \leq 4L[Q(x_{k-1}) + Q(\tilde{x})]. \tag{25}$$

Lemma 10. For any convex function R on $\mathbb{R}^D$, and $x, y \in \mathbb{R}^D$, it holds that

$$||prox_R(x) - prox_R(y)|| \leq ||x - y||. \tag{26}$$

Lemma 11. Suppose that Assumption 1 holds and each loss function is μ-strongly-convex. Then there exists $\gamma I \preceq H_k \preceq \Gamma I, \forall k \geq 1$ for OPDA-QN where $0 < \gamma < \Gamma$.

Remark 5. For OPDA-FM, there ia a constant $\gamma = \Gamma = 1$ since $H_k = I$. The bound for L-BFGS update can be found in [(Moritz, Nishihara, and Jordan 2016), Lemma 4] that

$$1/((D+M)L) \leq \gamma, \quad \Gamma \leq ((D+M)L)^{D+M-1}/\mu \tag{27}$$

and the bound for block L-BFGS update can be found in (Gower, Goldfarb, and Richtárik 2016), Lemma 1] that

$$1/(1+ML) \leq \gamma, \Gamma \leq (1+\sqrt{\alpha})(1+1/(2\sqrt{\alpha}\mu + \alpha\mu)). \tag{28}$$

where $\alpha = (1+\sqrt{L/\mu})^2$. For nonconvex problems, we may ajust the quasi-Newton methods as (Wang et al. 2017). Since we use the unaligned gradient during the BFGS update, this lemma still holds in our case, giving us a method of bounding the descent direction variance.

Lemma 12. For convex function R on $\mathbb{R}^D$, and $x, y \in \mathbb{R}^D$, $||\phi(x; z; \eta\lambda) - \phi(y; z; \eta\lambda)|| \leq ||x - y||$.

Remark 6. This is the non-expansiveness of OPDA based on a fixed reference orthant, resembling the property of proximal mapping in [(Rockafellar 2015) section 31].

Lemma 13. For any regularized function $P(x) = F(x) + R(x)$, where $F(x)$ is μ-strongly-convex and it has L-Lipschitz continuous gradient, $R(x)$ is convex, we define

$$x^- = x - \eta p, x^+ = \phi(x^-; x; \eta\lambda), q = \frac{1}{\eta}(x - x^+) \tag{29}$$

and define $p \in \mathbb{R}^D$, $g \in \mathbb{R}^D$, $\Delta \in \mathbb{R}^D$ by

$$g_i = \begin{cases} q_i, (\sigma(x_i^-)\sigma(x_i) = -1) \\ p_i, (\sigma(x_i^-)\sigma(x_i) \neq -1), \end{cases} \quad \Delta = g - \nabla F(x), \tag{30}$$

also define η as the stepsize that $0 < \eta \leq 1/L$, then for any $y \in \mathbb{R}^D$, $x \in \mathbb{R}^D$ and $x^+ \in \mathbb{R}^D$, we have

$$P(y) \geq P(x^+) + q^\top(y - x) + \frac{\eta}{2}||q||^2 + \frac{\mu}{2}||y - x||^2 + \Delta^\top(x^+ - y). \tag{31}$$

Lemma 14. Under the condition in Lemma 13, there is $||g|| \leq ||p||$ and $prox_{\eta R}(x - \eta g) = x^+$.

Remark 7. One can see that by viewing OPDA as a proximal algorithm, the second-order moment of the aligned direction g is smaller than p.

Suppose that the dataset is normalized, and each element has an expectation of zero, then the optimization trajectory $\{x_k\}_{k=0}^\infty$ is uniformly distributed in all orthants, therefore we have the following reasonable assumption.

Assumption 15. Suppose $x \in \mathbb{R}^D$ is a random point from the optimization trajectory of OPDA, each element of x has the same probability being positive or negative. For data samples S_k, the expectation of corresponding gradients is zero,

$$\mathbb{E}_{S_k}[\mathbb{E}_x[\nabla_i f_k(x)]] = \mathbb{E}_x[\nabla_i F(x)] = 0, \quad \forall i \in [D]. \tag{32}$$

Theorem 16. Suppose that Assumption 1 holds for each loss function f_n, then OPDA-FM in Algorithm 1 proceeds with a stepsize $0 < \eta < 1/(6L)$, the reference points $\{\tilde{x}_t\}_{t=1}^\infty$ converge to the global optima $x_\star$ in expectation, with a linear convergence rate, as

$$\mathbb{E}[Q(\tilde{x}_t)] \leq \left(\frac{2 + 8\mu L\eta^2(m+1)}{2\mu\eta(1-6L\eta)m}\right)^t Q(\tilde{x}_0). \tag{33}$$

Corollary 17. Suppose that Assumption 1 holds for each loss function f_n, then for OPDA-FM in Algorithm 1, by setting $\eta = \theta/L$, there is

$$\rho \approx \frac{L}{\mu\theta(1-6\theta)m} + \frac{4\theta}{(1-6\theta)}, \quad \mathbb{E}[Q(\tilde{x}_t)] \leq \rho^t \mathbb{E}[Q(\tilde{x}_0)],$$

if under appropriate settings that $m = \mathcal{O}(L/\mu)$ and θ is sufficiently small that $0 < \rho < 1$, then the iteration-complexity of attaining an ϵ-accurate suboptimum is

$$\mathcal{O}\left((N + \frac{L}{\mu})\log(\frac{1}{\epsilon})\right).$$

Remark 8. The convergence rate of OPDA-FM for strongly-convex function resembles that of Proximal-SVRG (Xiao and Zhang 2014). This is due to that the main techniques used in the analyses are both non-expansiveness.

Numerical Experiments

Logistic Regression

First, we implement OPDA in MATLAB, based on the code generously provided by the authors of (Gower, Goldfarb, and Richtárik 2016). We verify the algorithm's efficiency by logistic regression with L_2 and L_1 regularizations for binary classification task. The objective function is

$$P(x) = \frac{1}{N}\sum_n -\log[1 + \exp(-a_n^\top x b_n)] + \lambda_2||x||_2^2 + \lambda||x||_1, \quad a_n \in \mathbb{R}^D, \quad b_n \in \{-1, 1\}. \tag{34}$$

We use datasets from (Chang and Lin 2011), including **covtype** ($N = 581K, D = 54$) and **rcv1** ($N = 20K, D = 47K$). The regularization coefficients λ_1 and λ_2 are noted

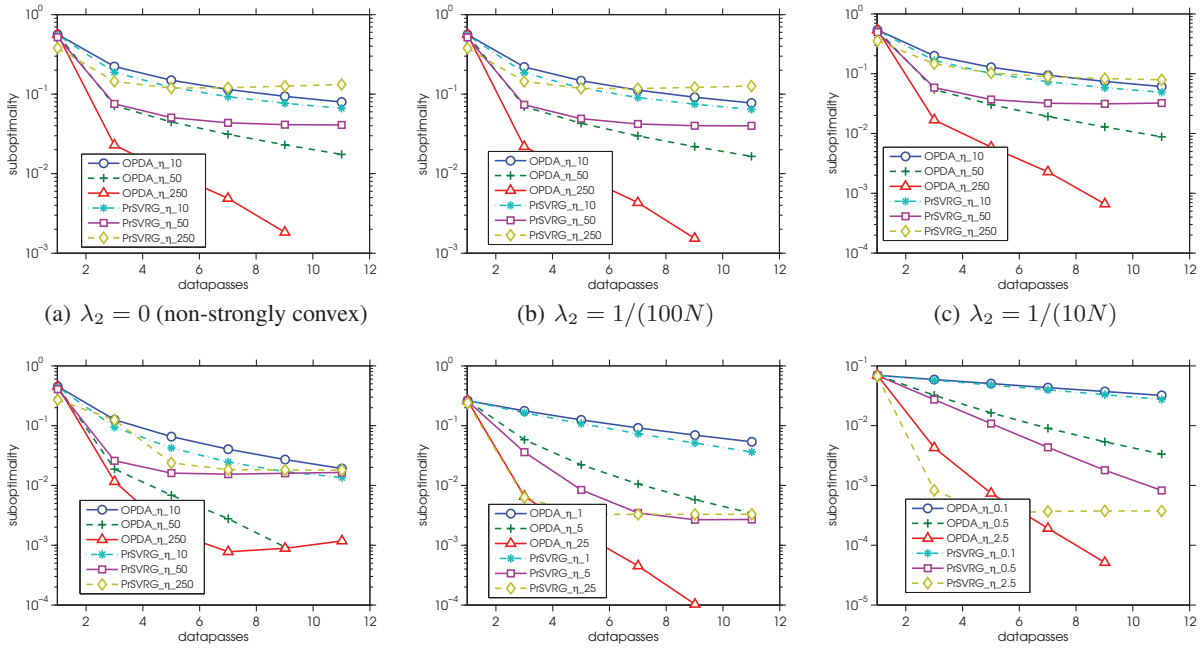

(a) $\lambda_2 = 0$ (non-strongly convex) (b) $\lambda_2 = 1/(100N)$ (c) $\lambda_2 = 1/(10N)$

(d) $\lambda_2 = 1/N$ (e) $\lambda_2 = 10/N$ (f) $\lambda_2 = 100/N$

Figure 3: Performance of OPDA-FM for different L_2 regularization on rcv1 dataset.

with the figures. If not noted, the default L_1 regularization is set to be $\lambda_1 = 10^{-5}\sqrt[4]{D}/\sqrt[4]{N}$ for rcv1 data, and $\lambda_1 = 10^{-5}$ for covtype; the default L_2 regularization for both datasets is set to be $\lambda_2 = 1/N$. We compare our algorithm (with a prefix **OPDA**) with the Proximal-SVRG algorithm (with a prefix **PrSVRG**). The stepsize η is noted after the prefix.

For OPDA and Proximal-SVRG, we use the same subsampling size $|\mathcal{S}_k| = \sqrt{N}$ for the gradient and Hessian update (for OPDA-QN). The stepsize is grid-searched for an optimum, whose nearby stepsizes are also tested and plotted. We set each outer iteration to consist of $m = N/|\mathcal{S}_k|$ times of inner iteration, during which both OPDA and Proximal-SVRG fully scan over the dataset before recalculating the full gradient and updating the reference point. We plot the convergence of OPDA-FM for strongly-convex problems (with L_2 and L_1 regularization) in [Figure 3: (bcdef)], and a non-strongly-convex problem (without L_2 regularization) in [Figure 3:(a)], where Y-axis shows the suboptimality $P(\tilde{x}_t) - P(x_\star)$ and X-axis shows data passes or running time. For rcv1, we set λ_2 and λ_1 to be different values, which are noted along with the figures. Figure 3 shows that OPDA-FM stably outperforms Proximal-SVRG, especially when the strong convexity coefficient μ is smaller; Figure 4 shows that the advantage of OPDA-FM over Proximal-SVRG is more prominent when the L_1 regularization is stronger.

For OPDA-QN, we set $M = 5$ as the memory size of curvature triples/pairs. The updating frequency of H_k also is also set to be M. We plot the suboptimality against the datapasses and the running time in Figure 5. The sampling strategies for Ξ_k are noted in the figure, like Guassian sampling as **gauss**, previous directions as **prev**, and Ξ_k being an identity matrix as **BFGS**. All OPDA-QN algorithms run considerably faster than Proximal-SVRG, by the advantages of second-order information. For low-dimensional data like covtype, OPDA-gauss, OPDA-prev strategies perform slightly different, but both outperform OPDA-BFGS, showing the effectiveness of the sketching technique. For high-dimensional data like rcv1, OPDA-BFGS perform faster than OPDA-prev, both in measure of data passes or running time, and they all outperform OPDA-gauss, since they consume less computations for calculating $d_k = H_k v_k$; and the running time per iteration of OPDA-BFGS is less than that of OPDA-prev. The acceleration of OPDA-QN in terms of data passes is very critical for modern machine learning applications. In the past decades, the computation power grew faster than the memory bandwidth, and this trend benefits OPDA-QN more, since QN type algorithms generally visit data less frequently by consuming more computations per iteration.

Deep Learning

We also conducted experiments with sparse convolutional neural networks for demonstrating nonconvex optimization efficiency and potential application in memory limited deep learning. For the consistency with other algorithms in the area, we use the stochastic gradient without variance reduction or quasi-Newton methods, so that $d_k = v_k = \diamondsuit f_k(x_{k-1})$. The algorithm is noted as OPDA-SGD. The network has three convolutional layers of $5 \times 5 \times 16$, $3 \times 3 \times 32$ and $3 \times 3 \times 48$ (kernel height, kernel width, output channels), three pooling layers of $(2, 2)$ (size, stride), a fully connected layer and a softmax loss layer. We use the **CIFAR10** dataset. The parameter of the network has L_1 regularization, whose coefficient λ is set to be $[10, \cdots, 10/2^7]$, and noted in

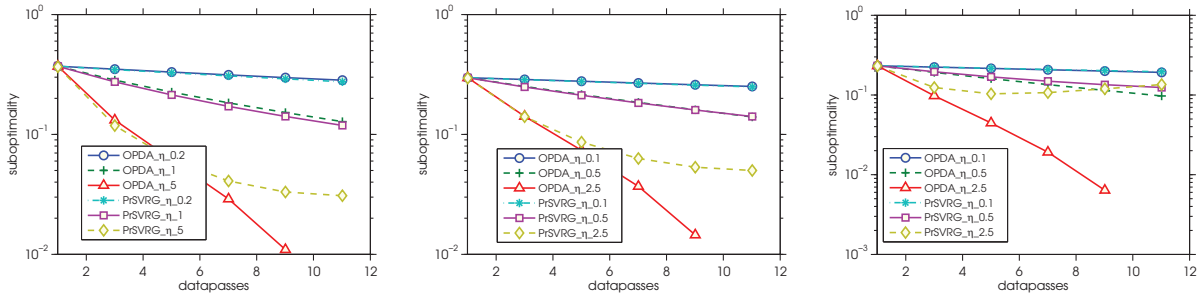

(a) $\lambda_1 = 4\bar{\lambda}_1$ (b) $\lambda_1 = 8\bar{\lambda}_1$ (c) $\lambda_1 = 32\bar{\lambda}_1$

Figure 4: Performance of OPDA-FM for different L_1 regularization on rcv1 dataset, $\bar{\lambda}_1 = 10^{-5}\sqrt[4]{D}/\sqrt[4]{N}$.

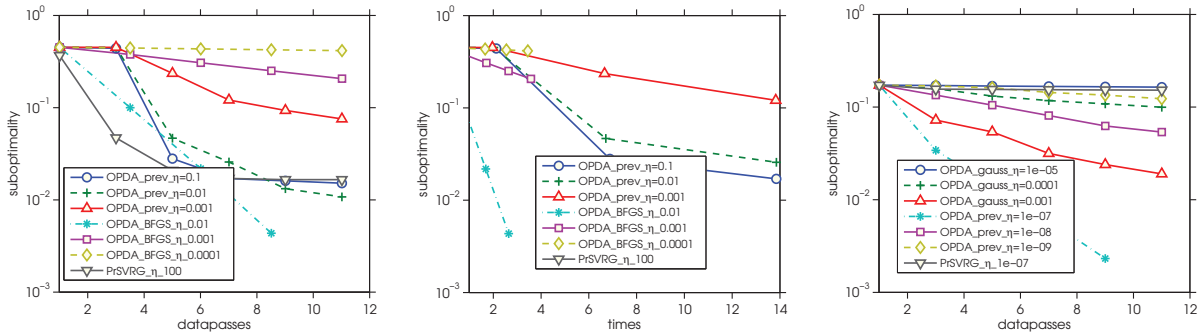

(a) $rcv1$ (b) $rcv1$ (c) $covtype$

Figure 5: Performance of OPDA-QN with different strategies and different datasets.

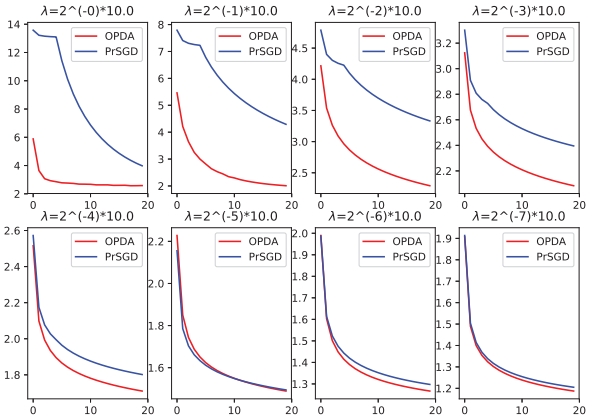

Figure 6: The performance of OPDA-SGD on CIFAR10. X-axis: datapasses; Y:axis: objective function.

the figure. We see that OPDA-SGD converges considerably faster than Proximal-SGD, as shown in Figure 6, especially when the L_1 regularization is stronger. This agrees with our intuition, since OPDA is specifically designed to tackle the strong non-differentiability.

In conclusion, as we see, although by the orthant-wise nature of OPDA, a large proportion of elements of the descent direction p and the updated parameter $x - \eta p$ are forced to zero during alignment, making the actual descent speed slower, OPDA-FM and OPDA-QN still converge much faster than state-of-the-art proximal algorithms, with the same stepsize. This proves that our proposed alignment operator does calibrate the direction to be a better one toward the optimum, making the algorithm considerably more efficient, with only negligible extra arithmetic operations consumed. In addition, OPDA-QN, with or without sketching, outperforms OPDA-FM under proper settings.

Conclusion

We propose OPDA as a good substitute of proximal algorithms to efficiently train L_1 regularized sparse models. We apply SVRG to initialize the descent direction, which can be calibrated by quasi-Newton methods (OPDA-QN). We propose a novel alignment operator to encourage the differentiability of the L_1 regularization. The parameter therefore cross each orthant passively during optimization. We prove a linear convergence rate of the algorithm with strong convexity and smoothness, and the experiments show that OPDA stably and significantly outperforms proximal algorithms on both convex and nonconvex problems.

References

Andrew, G., and Gao, J. 2007. Scalable training of ℓ_1-regularized log-linear models. In *Proceedings of the 24th International Conference on Machine learning*, 33–40. ACM.

Bach, F.; Jenatton, R.; Mairal, J.; Obozinski, G.; et al. 2012. Optimization with sparsity-inducing penalties. *Foundations and Trends® in Machine Learning* 4(1):1–106.

Bottou, L. 2010. Large-scale machine learning with stochastic gradient descent. In *Proceedings of COMPSTAT'2010*. Springer. 177–186.

Bühlmann, P., and Van De Geer, S. 2011. *Statistics for high-dimensional data: methods, theory and applications*. Springer Science & Business Media.

Byrd, R. H.; Hansen, S.; Nocedal, J.; and Singer, Y. 2016. A stochastic quasi-newton method for large-scale optimization. *SIAM Journal on Optimization* 26(2):1008–1031.

Candes, E., and Tao, T. 2007. The dantzig selector: Statistical estimation when p is much larger than n. *The Annals of Statistics* 2313–2351.

Chang, C.-C., and Lin, C.-J. 2011. LIBSVM: a library for support vector machines. *ACM Transactions on Intelligent Systems and Technology (TIST)* 2(3):27.

Defazio, A.; Bach, F.; and Lacoste-Julien, S. 2014. SAGA: A fast incremental gradient method with support for non-strongly convex composite objectives. In *Advances in Neural Information Processing Systems*, 1646–1654.

Efron, B.; Hastie, T.; Johnstone, I.; Tibshirani, R.; et al. 2004. Least angle regression. *The Annals of statistics* 32(2):407–499.

Friedman, J.; Hastie, T.; and Tibshirani, R. 2001. *The elements of statistical learning*, volume 1. Springer series in statistics New York.

Gong, P., and Ye, J. 2015a. HONOR: Hybrid optimization for non-convex regularized problems. In *Advances in Neural Information Processing Systems*, 415–423.

Gong, P., and Ye, J. 2015b. A modified orthant-wise limited memory quasi-newton method with convergence analysis. In *Proceedings of the 32nd International Conference on Machine Learning*, 276–284. ACM.

Gower, R.; Goldfarb, D.; and Richtárik, P. 2016. Stochastic block BFGS: squeezing more curvature out of data. In *Proceedings of the 33rd International Conference on Machine Learning*, 1869–1878. ACM.

Johnson, R., and Zhang, T. 2013. Accelerating stochastic gradient descent using predictive variance reduction. In *Advances in Neural Information Processing Systems*, 315–323.

Liu, D. C., and Nocedal, J. 1989. On the limited memory BFGS method for large scale optimization. *Mathematical Programming* 45(1):503–528.

Luo, L.; Chen, Z.; Zhang, Z.; and Li, W.-J. 2016. A proximal stochastic quasi-newton algorithm. *arXiv preprint arXiv:1602.00223*.

Mokhtari, A., and Ribeiro, A. 2014. RES: Regularized stochastic BFGS algorithm. *IEEE Transactions on Signal Processing* 62(23):6089–6104.

Moritz, P.; Nishihara, R.; and Jordan, M. 2016. A linearly-convergent stochastic L-BFGS algorithm. In *Proceedings of the 19th International Conference on Artificial Intelligence and Statistics*, 249–258.

Nesterov, Y. 2013. *Introductory lectures on convex optimization: A basic course*, volume 87. Springer Science & Business Media.

Nocedal, J., and Wright, S. J. 1999. Numerical optimization. *Springer Science* 35(67-68):7.

Parikh, N.; Boyd, S.; et al. 2014. Proximal algorithms. *Foundations and Trends® in Optimization* 1(3):127–239.

Reddi, S. J.; Sra, S.; Póczos, B.; and Smola, A. J. 2016. Proximal stochastic methods for nonsmooth nonconvex finite-sum optimization. In *Advances in Neural Information Processing Systems*, 1145–1153.

Rockafellar, R. T. 2015. *Convex analysis*. Princeton university press.

Schraudolph, N. N.; Yu, J.; Günter, S.; et al. 2007. A stochastic quasi-newton method for online convex optimization. In *Proceedings of the 10th International Conference on Artificial Intelligence and Statistics*, volume 7, 436–443.

Shalev-Shwartz, S., and Zhang, T. 2014. Accelerated proximal stochastic dual coordinate ascent for regularized loss minimization. In *Proceedings of the 32nd International Conference on Machine Learning*, 64–72.

Shamir, O., and Zhang, T. 2013. Stochastic gradient descent for non-smooth optimization: Convergence results and optimal averaging schemes. In *Proceedings of the 30th International Conference on Machine Learning*, 71–79. ACM.

Wang, X.; Ma, S.; Goldfarb, D.; and Liu, W. 2017. Stochastic quasi-newton methods for nonconvex stochastic optimization. *SIAM Journal on Optimization* 27(2):927–956.

Xiao, L., and Zhang, T. 2014. A proximal stochastic gradient method with progressive variance reduction. *SIAM Journal on Optimization* 24(4):2057–2075.

Yu, J.; Vishwanathan, S.; Günter, S.; and Schraudolph, N. N. 2010. A quasi-newton approach to nonsmooth convex optimization problems in machine learning. *Journal of Machine Learning Research* 11(Mar):1145–1200.

Zhang, T. 2004. Solving large scale linear prediction problems using stochastic gradient descent algorithms. In *Proceedings of the 21st International Conference on Machine learning*, 116. ACM.

Zhang, T. 2011. Adaptive forward-backward greedy algorithm for learning sparse representations. *IEEE Transactions on Information Theory* 57(7):4689–4708.